University of Groningen

The organic ties of iron

Slagter, Hans Arent

IMPORTANT NOTE: You are advised to consult the publisher's version (publisher's PDF) if you wish to cite from it. Please check the document version below.

Document Version
Publisher's PDF, also known as Version of record

Publication date:
2018

Link to publication in University of Groningen/UMCG research database

Citation for published version (APA):
Slagter, H. A. (2018). *The organic ties of iron: Or the origin and fate of Fe-binding organic ligands*. [Thesis fully internal (DIV), University of Groningen]. Rijksuniversiteit Groningen.

Chapter 8

Effects of viral lysis and dark-induced senescence of phytoplankton on Fe-binding organic ligand production and composition

Abstract

Low-Fe adapted cultures of *Micromonas pusilla* and *Phaeocystis globosa* infected by their specific viruses (PgV-07T and MpV-08T) showed highest ligand concentrations only for the infected *P. globosa*. Conditional ligand binding strength was also higher for *P. globos*a, but more so for the control than the infected cultures. An inventory of siderophore-like substances yielded as of yet unknown Gallium (Ga) complexes in all treatments, i.e. controls, infected and 30 day dark-induced senesced phytoplankton. These complexes possibly represent siderophore-like substances. We found changes in the composition of these siderophore-like substances due to bacterial presence, in cases irrespective of the phytoplankton host and treatment. Ga-complex signature types unique to samples post senescence period suggest that heterotrophic bacteria are a possible source of specific Fe-binding organic ligands. Loss of Ga-complex signature types detected before the senescence period suggests that dissolved Fe-binding organic ligands within this group are subject to bacterial uptake and modification in addition to ligand production. An overall loss in Ga-complex ion counts would suggest these processes are a loss factor of Fe-binding organic ligands over time. Ultimately, both viral lysis and senescence of phytoplankton and viral lysis thereof act on the Fe-binding organic ligand pool as both sources and loss factors.

8.1. Introduction

Marine phytoplankton form the base of most marine foodwebs and play a key role in sequestration of atmospheric carbon. Phytoplankton production is regulated by growth-relevant environmental variables, so called bottom-up control factors. Amongst these, the trace metal iron (Fe) has been shown to limit phytoplankton growth in vast oceanic regions (de Baar et al., 1990; Martin et al., 1990). Fe is an essential nutrient for enzymes involved in DNA replication, electron transport in photosynthesis and cellular respiration, , the reduction of reactive oxygen and the nitrogen cycle (Geider and La Roche, 1994; Hogle et al., 2014; Zhang, 2014; de Baar et al., 2017). However, organic Fe-binding ligands are required to keep Fe in the bioavailable dissolved state beyond inorganic solubility (Liu and Millero, 2002). The vast majority of dissolved Fe is bound to organic ligands, yet the identity of these ligands is still largely unknown (Gledhill and Buck, 2012; Hassler et al., 2017).

Fe-binding organic ligands in marine systems may originate from terrestrial sources as humic substances (Laglera and van den Berg, 2009), but may also be produced locally in biologically active regions (Rue and Bruland, 1995; Gerringa et al., 2006). Viral lysis of a unicellular host releases the cytosol directly into the surrounding seawater, delivering carbon and nutrients in bioavailable forms. Subsequent bacterial remineralisation mobilizes these nutrients in the microbial food web (Brussaard et al., 2005; Suttle, 2005). Viral lysis of phytoplankton has been shown to increase the release of dissolved iron (Gobler et al., 1997). What is as nevertheless still unknown is to what extent phytoplankton lysis specifically contributes to the ligand pool. Poorvin et al. (2011) showed that viral lysis of marine bacteria contributed to the ligand pool, and the Fe in these viral lysates seemed well bioavailable (Mioni et al., 2005; Poorvin et al., 2011).

The Fe-binding ligand pool is modified by bacterial activity not only via microbial consumption of virally-released ligands, but also of ligands from exudates such as exopolymeric substances (EPS; Hassler et al., 2011b, 2011a) and those associated with terrestrial produced organic matter (Laglera and van den Berg, 2009). Alternatively, bacteria produce ligands via production of siderophores (Butler, 2005; Hassler et al., 2017). Siderophores are a long-studied subject, with the first examples isolated from soils by Francis et al. (1949), before their relevance in marine systems became apparent following the iron hypothesis (Martin and Fitzwater, 1988). Since then siderophores have been purposefully produced as metal chelators, i.e. for medical purposes, and have been studied in their role as Fe mobilizers for (cyano-)bacteria (Wilhelm and Trick, 1994; Butler, 2005; Hopkinson et al., 2009) and their possible utilization as Fe sources

for phytoplankton directly (Soria-Dengg et al., 2001). Enzymes tied to high-affinity Fe-uptake systems and siderophore-specific genes have been detected in phytoplankton species before (Wilhelm et al., 2006). *In situ* studies of siderophore production have shown that specific siderophores drive bioavailability of Fe (Velasquez et al., 2011, 2016). However, siderophore characterization is incomplete and relative contribution to the dissolved organic Fe-binding ligand pool is unknown. Modification of the Fe-binding organic ligand pool has been indicated indirectly via multiple avenues (Rijkenberg et al., 2008a; Boyd et al., 2010). The growth of heterotrophic bacteria supported by the processes described above is expected to be a loss factor to Fe-binding organic ligands.

Here we investigate the role of viral lysis of two cosmopolitan phytoplankton species, *Micromonas pusilla* and *Phaeocystis globosa*, in dissolved organic Fe-binding ligand production and composition. Furthermore, the influence of bacterial breakdown of the virally lysed phytoplankton cells as well as dark-induced senescence of the non-infected phytoplankton during a 4 week period.

8.2. Method

8.2.1. Model systems

Phytoplankton species used were the picoeukaryotic prasinophyte *Micromonas pusilla* (LAC38, Marine Research Center culture collection, Göteborg University, Sweden) and the nanoeukaryotic Prymnesiophyte *Phaeocystis globosa* (G(A); culture collection of the University of Groningen, the Netherlands). Monospecific cultures of each were cultured in a low-trace metal (LT) medium containing no added complexing agents after Slagter et al. (2016). The double stranded DNA algal viruses MpV-08T infecting *M. pusilla*(Martinez Martinez et al., 2015) and PgV-07T infecting *P. globosa* (Baudoux and Brussaard, 2005) were maintained by regular transfer (10% v/v) of the lysates to new exponentially growing algal cultures (in LT medium).

8.2.2. Experimental design, sampling and abundance analysis

Prior to the infection experiment, phytoplankton cultures were scaled up to 2 L in PC vessels (Nalgene). Following, phytoplankton were transferred to 10 L PC carboys (Nalgene). The exponentially growing phytoplankton were each split into two batches that served as non-infected controls and two batches that were inoculated with the specific virus (10% v/v). Experiments started with an average host abundance of 7.1×10^5 mL^{-1} (SD=1.0, N=4) for *P. globosa* and 1.4×10^6 mL^{-1} (SD=0.1, N=4) for *M. pusilla*. Samples for flow cytometric enumeration of phytoplankton, bacteria and viruses, and samples for photosynthetic capacity (F_v/F_m) were taken at regularly until 96 h post infection

(p.i.). Phytoplankton abundances were directly determined using a FACSCanto flow cytometer (Becton Dickinson) equipped with a 12 mW HeNe laser (633 nm) with the trigger set on Chlorophyll-a red autofluorescence. The measurements for F_v/F_m were also performed on fresh samples using a fluorometer with Chlorophyll red detector (Waltz Water-PAM), whereby triplicate readings were taken after 30 min dark equilibration at culturing temperature. Samples for bacterial and virus abundances were fixed with glutaraldehyde to a final concentration of 0.5 % (EM grade, 25% stock, Merck) and subsequently flash frozen in liquid N_2 (Brussaard, 2004b). Samples were stored at -80°C until analysis using a FACSCalibur flow cytometer (Becton Dickinson, equipped with a 15 mW 488nm argon-ion laser). Prior to analysis the samples were diluted in TE-buffer and stained with nucleic acid specific dye SYBR Green I (Thermo Fisher) according to Brussaard et al. (2010). The algal viruses were differentiated on a green fluorescence versus side scatter cytogram. All flow cytometric data were analysed in detail using Cytowin (Vaulot, 1989).

Samples for the determination of DFe and ligand characteristics were taken at 0, 24, 50, 76 and 96 h p.i. Trace metal speciation samples were selected based on contamination and/or difficulties with electrochemical measurements in culture filtrates. Only samples with a DFe within 1nM of the LT medium's target of 3nM and for which a fit to the Langmuir model was possible were retained. All samples that remained were taken between 50 and 96 h p.i., ultimately representing all treatment end-states. Samples for siderophore analysis were taken at 96 h p.i. Following these samplings, the cultures were left in the dark for approximately 4 weeks (30 days) to study the effect of bacterial degradation of organic matter on additional samples for siderophore analysis. Samples taken after the 30 d senescence period could not be analysed for Fe-binding organic ligands due to electrochemical interference. Successful senescense of the phytoplankton cultures was verified with flow cytometery. All samples for DFe, ligand characteristics and siderophore analysis were filtered using a PC overpressure filtration system with a 0.2 μm polyethersulfone (PES) filter (Vivacell 250, Sartorius). This system, using a vertically oriented filter cup with minimal deadspace, was placed on an orbital shaker at mild velocity to minimize filter clogging. Pressure over the unfiltered sample (no vacuum) was kept to ~2 bar, minimalizing the potential for mechanical cell lysis.

8.2.3. Trace metal analyses

DFe samples were concentrated on a chelating column (NOBIAS chelate-PA1) using an automated sample preconcentration system (seaFAST, Elemental Scientific). 10 mL acidified seawater (0.024 M HCl; BASELINE, Seastar) was concentrated and eluted in 1 mL 1.5 M 2x SBD HNO_3, and subsequently

measured by high resolution inductively coupled plasma mass spectrometry (HR ICP-MS; Element2, Thermo Scientific). Calibration was performed by standard addition using diluted 1000-ppm stock solutions (TraceCERT for ICP, Fluka).

Ligand concentration ($[L_t]$ in equivalent nM of Fe (Eq. nM Fe)) and conditional binding strengths relative to Fe' ($logK'_{Fe'L}$, in mol^{-1}) were measured using competitive ligand exchange adsorptive cathodic stripping voltammetry (CLE-AdCSV). The competitive ligand salicydiaxomine (SA) was used in a concentration of 25 µM after Buck et al. (2007, 2015).

Siderophore analyses were performed after Mawji et al. (2008). Samples for siderophore analysis were preconcentrated onto hydroxylated polystyrene-divinyl benzene copolymer solid phase extraction columns (Isolute ENV+, Biotage) using a tubing pump (Ismatec). Tubing (Tygon®, Saint-Gobain) was first flushed with ~500 mL 1 M HCl (Normapur, VWR) followed by ~500 mL MQ at 10 mL min^{-1}. Columns were preconditioned with ~10 mL SBD methanol, followed by ~100 mL MQ at 3 mL min^{-1}. An average 923±48 mL sample was passed over the cartridges with exact volumes per sample registered for calculation of preconcentration factors. Cartridges were then stored at -18 °C prior to liquid chromatography. Before analysis the cartridges were washed with 5 mL 10 mM $(NH_4)_2CO_3$ and siderophores eluted with 84:14:5:0.1 (v:v:v:v) acetonitrile: propan-2-ol: MQ: NH_4formate. 2 mL eluant was reduced to ~100 µL by vacuum centrifuge at room temperature (SpeedVac, Thermo Scientific). Finally, 500 µL 5 mM NH_4formate was added to the reduced eluant, bringing the final volume to ~600 µL. Samples were divided into 5 aliquots. Aliquot 1 was analysed directly, aliquots 2, 3 and 4 were spiked with 0.5 mM $FeCl_3$ (made fresh from $FeCl_3.6H_2O$, Carl Roth) and aliquots 3 and 4 with ferrioxamines B, E (Sigma) and ferrioxamine G (EMC microcollections) to create a standard addition curve for the quantification of the respective ferrioxamine siderophores. Detection limits for ferrioxamine B, G and E were 0.4, 15.3 and 0.6 nmol L^{-1} respectively in the analysed solutions. Aliquot 5 was spiked with 10000 ppm Ga solution (final concentration 5mM Ga, VWR) and left overnight at room temperature before analysis.

Separation of siderophore-like substances was performed using a biocompatible UltiMate 3000 high-performace liquid chromatography (HPLC) system (Thermo Scientific), equipped with a poly styrene-divinylbenzene column (PRP H1, Hamilton; 5 µm 2.1 x 100 mm). Solvent A was 5% methanol and 5 mM ammonium formate (both Optima LC-MS, Fisher) in MQ (pH 5.8); solvent B was 100% methanol. The gradient spanned 15 minutes from 0 to 100% of solvent B, followed by 5 more minutes of solvent B. The column was then re-equilibrated to starting conditions. The flow rate was 400 µL min^{-1}. Separated samples were

passed to a hybrid quadrupole-orbitrap mass spectrometer (Q Exactive, Thermo Scientific) in +ve ion mode with a scan range of m/z 300-1500.

Chromatography data was was mined for the Ga isotopic ratio using Chelomex (Baars et al., 2014) after conversion to mzXML format using MSconvert (ProteoWizard; Kessner et al., 2008). A master list of potential Ga complexes was compiled, and monoisotopic masses for the uncharged metal free form of the molecule calculated (M), assuming the detected Ga isotopes were ionized as the $(M-2H+Ga)^+$ ion. Masses for $(M-2H+Fe)^+$, $(M-2H+^{69}Ga)^+$, $(M+H)^+$ and $(M+Na)^+$ were then calculated and chromatograms obtained from analysing aliquot 1 were mined for the corresponding masses in MZmine using an m/z tolerance of 10 ppm and a retention time tolerance of ±2 min with respect to the retention time of the $(M-2H+Ga)^+$ peak (Pluskal et al., 2010). The mined masses were filtered to remove duplicates and peaks with areas $<5×10^5$ ion counts[2]. Finally, mass spectra for each putatively identified peak were examined for isotopic consistency and a list of peak m/z, retention times and peak areas produced. Graphics were produced in R (R Development Core Team, 2008).

8.3. Results

8.3.1. Growth characteristics

While the non-infected control cultures of *M. pusilla* and *P. globosa* showed expected growth during the experimental period (96 h), the infected cultures displayed a steady decline in abundances after about 1 day p.i. (Figure 1A, B). The duplicate infected *M. pusilla* cultures showed some discrepancies the second day of the experiment, whereby one of the replicates still mimicked the control abundances while the other already showed halted growth. The F_v/F_m values showed for *M. pusilla* a similar temporal dynamics as the algal abundances, whereas for *P. globosa* the decline in F_v/F_m occurred quickly upon infection (Figure 1C, D). Full lysis of the infected algal cultures was obtained after 72 h for *M. pusilla* and 60h for *P. globosa*. The latent period of the algal viruses, i.e. the time the abundance of extracellular viruses started to increase, was between 12-16 h and 8-12 h for MpV-08T an PgV-07T, respectively (Figure 1E, F).

Usable samples for Fe speciation characteristics represented the time cell lysis of the infected *M. pusilla* was halfway and almost complete for the infected *P. globosa* (50 h p.i.), and cell lysis was complete (76 h, 96 h p.i.).

8.3.2. Fe speciation characteristics

Ligand concentrations ($[L_t]$, Table 1, Fig. 2A) were not dissimilar for *M. pusilla* treatments with the exception of one high outlier in one replicate of the infected cultures (M3, 22.98 Eq. nM Fe at 76 h p.i.). The L_t concentrations in the *P.*

globosa control cultures were similar to the *M. pusilla* cultures, overall 11.78±1.49 Eq. nM Fe minus the outlier in infected *M. pusilla* above (N=10, see table 1). In the infected *P. globosa* cultures $[L_t]$ was much higher at 17.75±0.60 Eq. nM Fe (N=3). This difference was reflected similarly in the free ligand concentration (L'), which represents the fraction of $[L_t]$ that is available to bind additional Fe beyond the dissolved Fe concentration (DFe). If we normalize $[L_t]$ to cytosol volume, assuming a cell radius of 1.5 μm for *M. pusilla* and 2 μm for *P. globosa*, the differences between host species are no longer present, with standard deviations between all treatments overlapping for an average 612.23±123.52 Eq. nM Fe μm^{-3}. Here again M3 at 76 h p.i. is an outlier (1185.84 Eq. nM Fe μm^{-3}) omitted from the average.

The conditional binding constant of *M. pusilla* cultures was also not significantly different between treatments (Fig. 2B). The logK'$_{Fe'L}$ values for *P. globosa* controls were higher than for *M. pusilla*, but less so for the infected cultures of *P. globosa*. This was again similarly reflected in the reactivity value (logα$_{Fe'L}$), which is defined as the product of K' and L'. We find mean logα$_{Fe'L}$ values of 4.11±0.37 for *M. pusilla* and 4.81±0.34 for *P. globosa* (Fig. 2C).
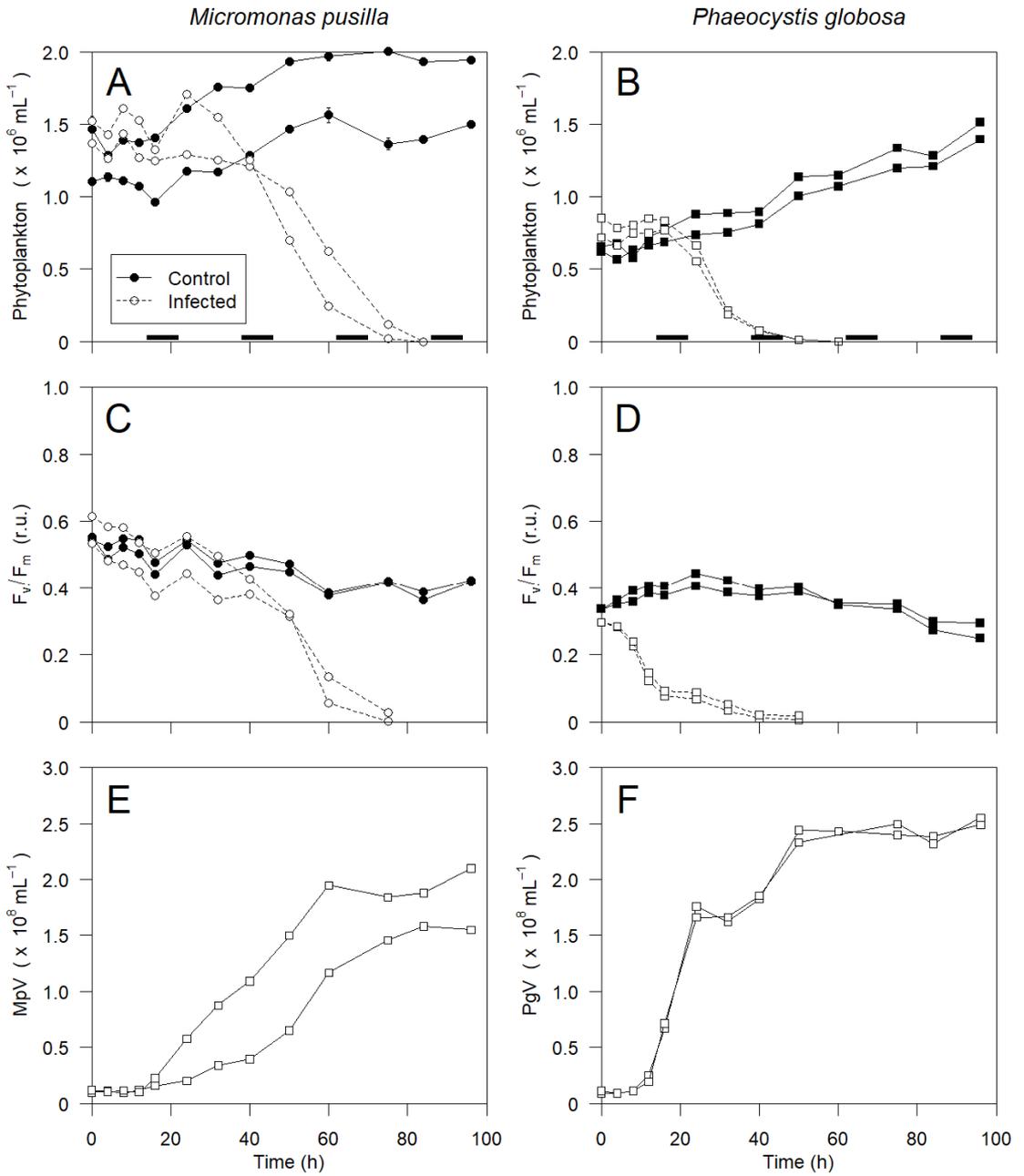
Figure 1   Temporal dynamics of *P. globosa* (A) and *M. pusilla* (B), F_v/F_m (C, D), MpV (E) and PgV (F). Black bars indicate dark periods. Duplicate cultures are shows separately in each graph. Error bars represent standard error of the mean of duplicate measurements (A, B, E-H) or triplicate measurements (C-D); where not visible these fall behind the symbols.

Table 1

Dissolved Fe (DFe) and Fe speciation characteristics for those samples that could successfully be analysed electrochemically. Reported here are the conditional binding strength of the ligands ($logK'_{Fe'L}$) with standard error, the total ligand concentration [L_t] with standard error, the excess ligand concentration [L'] and the reactivity of the ligands ($log\alpha_{Fe'}$).

|	Code	T	DFe	$logK'_{FeL,Fe'}$	SE	[L_t]	[L_t] SE	[L']	$log\alpha_{Fe'}$
		h p.i.	nM	mol^{-1}	mol^{-1}	Eq. nM Fe	Eq. nM Fe	Eq. nM Fe	
M. pusilla	M2	50	1.99	12.47	0.34	10.05	0.36	8.06	4.38
control	M1	76	2.65	12.33	0.33	13.10	0.66	10.45	4.35
	M1	96	2.97	11.69	0.12	10.95	0.38	7.98	3.59
	M2	96	2.27	12.43	0.24	13.07	0.22	10.80	4.46
M. pusilla	M3	50	2.92	11.75	0.42	13.20	1.01	10.28	3.76
infected	M4	50	2.29	12.44	0.54	10.71	0.90	8.42	4.36
	M3	76	3.24	12.16	0.39	22.98	1.01	19.74	4.45
	M4	76	1.34	11.60	0.23	11.25	0.70	9.91	3.59
	M4	96	2.39	12.14	0.39	9.92	0.34	7.53	4.02
P. globosa	P1	50	3.72	13.31	0.54	13.02	0.30	9.30	5.28
control	P2	50	1.66	12.88	0.51	9.49	0.35	7.83	4.77
P. globosa	P3	50	3.34	12.44	0.34	17.50	0.42	14.16	4.59
infected	P4	50	1.43	12.79	0.66	17.32	0.66	15.89	4.99
	P4	76	1.43	12.19	0.19	18.43	0.28	17.00	4.42
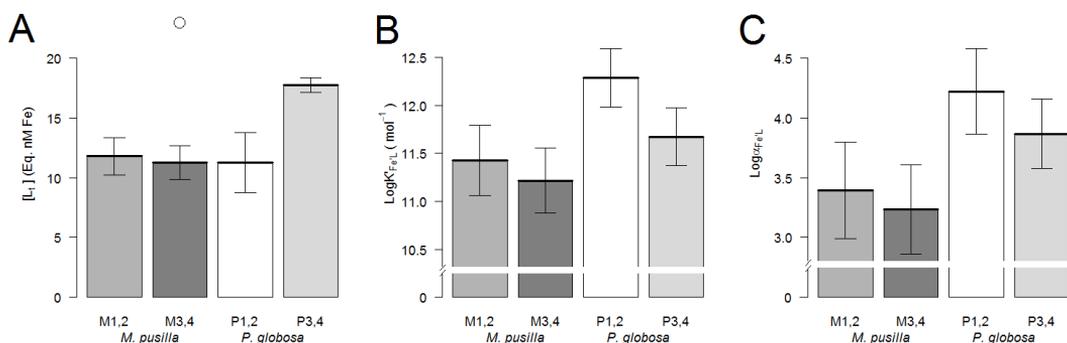
Figure 2 Fe speciation characteristics for selected samples as shown in Table 1: *M. pusilla* controls (M1,2) and infected (M3,4), *P. globosa* controls (P1,2) and infected (P3,4). A) Ligand concentration [L_t], B) conditional binding constant (LogK'$_{Fe'L}$) and C) reactivity (Logα$_{Fe'L}$).

Ferrioxamine B, G and E concentrations were quantified at the end of the experiment (96 h p.i.) and after the 30-day senescence period (Table 2). Very few ferrioxamines could be resolved in *M. pusilla* cultures at 96 h p.i. However, concentrations in the senesced controls had increased just above the detection limit. Contrastingly, ferrioxamines in *P. globosa* cultures occurred in the highest concentrations at 96 h p.i., particularly FOG. FOG was largely undetectable after 30 days.

A further 21 ions with distinctive Ga isotopes were identified in the samples. For one of these ions (m/z [69]Ga isotope = 769.327, retention time = 6.92), the corresponding [56]Fe mass was detected after Fe addition (m/z = 756.335, retention time = 6.85, see Figure S1, page 174). The highest number of compounds was observed in the *P. globosa* controls (24 in P1 control and 21 in the P2 control). The three Ga ions observed in P1 but not in any other treatments included Ferrioxamine E, m/z([69]Ga) 769.327 and m/z([69]Ga) 727.279. Three ions (m/z [69]Ga isotope = 386.109, 414.104 and 521.020) were common to all treatments. Viral infection resulted in a reduction of ions exhibiting Ga isotopic signatures for *P. globosa* samples, but not for *M. pusilla* samples. Allowing the cultures to senesce for 30 days resulted in a reduction of the number of ions exhibiting Ga isotopic signatures for all treatments and species (Figure 3).

Table 2	Ferrioxamine B (FOB), G (FOG) and E (FOE) concentrations in pM in samples at the end of the infected cultures' lytic cycle (T = 96 h p.i.) and after a 30-day senescence period (T = 30 d p.i.). Measurements under the detection limit are denoted "<dl" in grey.

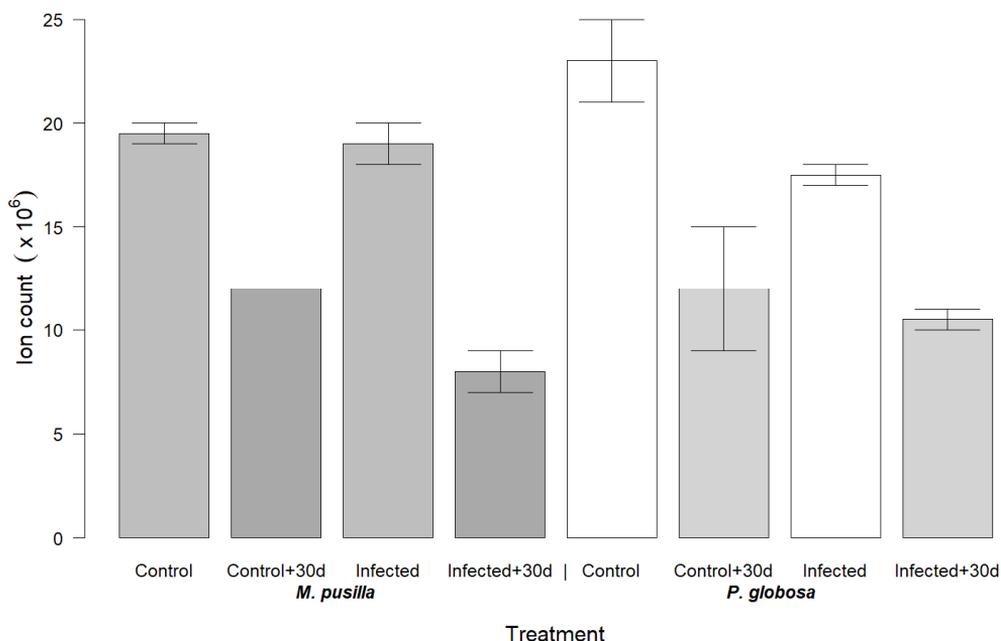|	T = 96 h				T = 30 d			
	Controls		Infected		Controls		Infected	
M. pusilla	M1	M2	M3	M4	M1	M2	M3	M4
FOB (pM)	<dl	<dl	<dl	2.6	2.3	13.5	<dl	1.6
FOG (pM)	<dl	<dl	<dl	<dl	<dl	9.2	<dl	<dl
FOE (pM)	2.7	<dl	<dl	<dl	4.7	<dl	<dl	<dl
P. globosa	P1	P2	P3	P4	P1	P2	P3	P4
FOB (pM)	<dl	0.8	0.7	<dl	<dl	<dl	0.8	<dl
FOG (pM)	747	35	33	20	<dl	<dl	10	<dl
FOE (pM)	9.5	<dl	<dl	<dl	1.5	<dl	<dl	<dl

Figure 3 Peak surfaces pooled for 21 detected mass ratios (m/z) for Ga isotopic signatures detected in *M. pusilla* and *P. globosa* treatments at 96 h p.i., and after 30 days senescence (+30d).
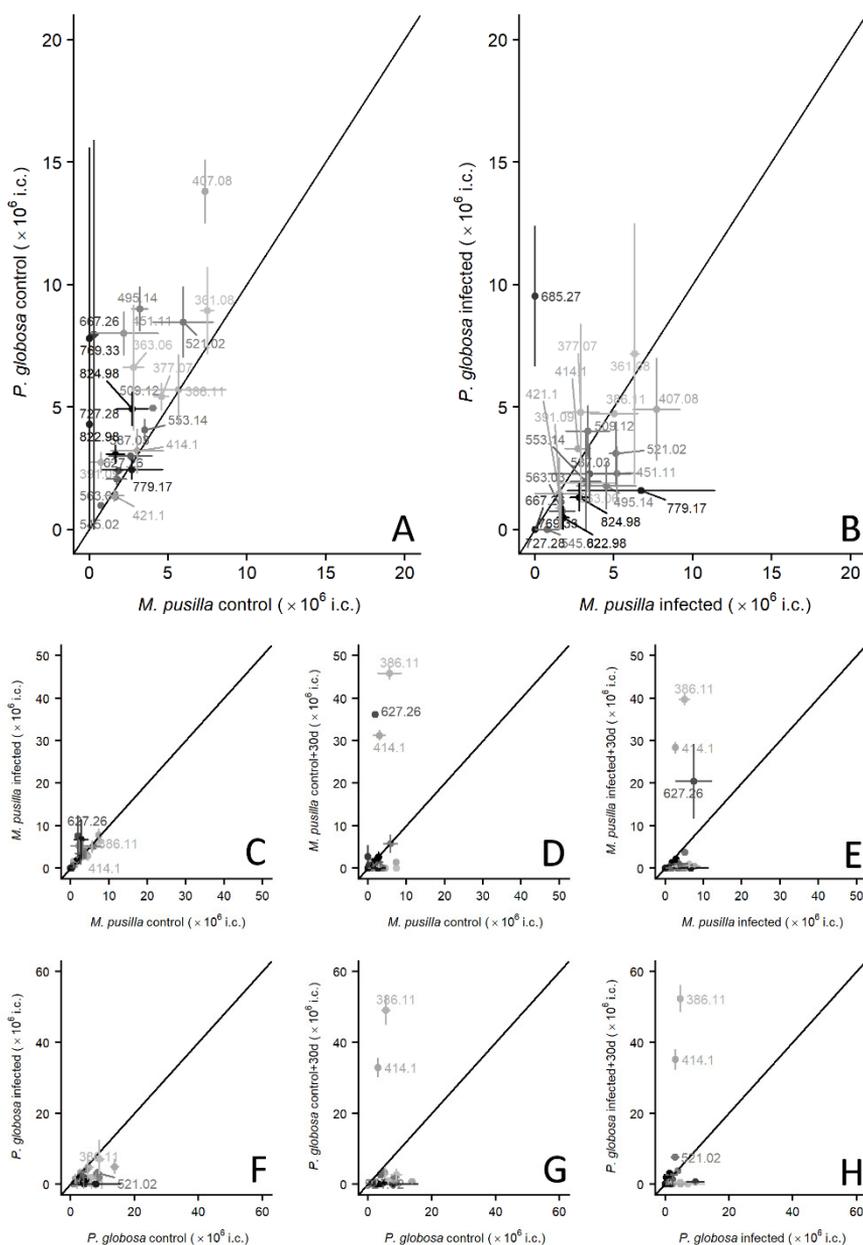
Figure 4 Comparison of peak surfaces for discrete mass ratios (m/z, values with points) for Ga isotopic signatures for A) all *P. globosa* controls against all *M. Pusilla* controls, B) all *P. globosa* infected against all *M. Pusilla* infected. Then for *M. pusilla*: C) infected vs. controls, D) controls after senescence vs. controls at 96 h p.i., E) infected after senescence vs. infected at 96 h p.i.; followed by the same 3 plots for *P. globosa* (F-H). Datapoints are greyed from high (black) to low (light grey) for contrast. Axes represent ion count (i.c.).

168

Comparison of the ion count registered with Ga isotopic signatures between species (Figure 4A) showed that the concentration of identified ions was higher in *P. globosa* controls than in *M. pusilla* control cultures, although there was considerable variability in ion count between the replicates. This difference between the algal species was not preserved in infected cultures (Figure 4B). The abundance of the putative Ga ions was similar or decreased slightly in infected samples. However, two ions (m/z 386.11 and 414.10) consistently increased in abundance by an order of magnitude in the samples allowed to senesce (Figure 4D-H). In *M. pusilla* cultures, ion counts of these two ions were within an order of magnitude of those observed for the ^{69}Ga complex of desferrioxamine B (m/z 627.267, Figure 4D, E).

8.4. Discussion

In absolute terms, the virally-infected *P. globosa* cultures showed the highest ligand concentrations, which would indicate that viral lysis of phytoplankton can enhance the concentration of ligands, to our knowledge not shown before the present study. However, when normalizing [L_t] to the cytosol volume, the errors again overlap. Lysates of *M. pusilla* did not seem to show a net effect of lysis in mean [L_t] values; however, one of the *M. pusilla* lysate replicates did show high [L_t] which remained significantly high after normalisation to cytosol volume.

The mean ligand binding strengths (logK'$_{Fe'L}$) were lower for the *P. globosa* lysates than for the controls, which implies that different types of ligands are released by virally lysed cells and senesced cultures. However, logK'$_{Fe'L}$ varies with host species and it cannot be excluded that the difference was due to differences in the bacterial activity and community composition between the control and infected cultures. Earlier studies have shown a rapid increase in bacterial production to viral lysis of *P. globosa*, which major shifts in the community composition (Brussaard et al., 2005; Sheik et al., 2014). logK'$_{Fe'L}$ values fall in the ranges associated with siderophore presence, at a mean 12.07 ± 0.34 mol^{-1} for *M. pusilla* and 12.72 ± 0.43 mol^{-1} for *P. globosa*.

Prior reported measurements of viral lysates of bacteria (Poorvin et al., 2011), LogK'$_{Fe3+}$ of 20.08 ± 0.58 mol^{-1} were found using CLE-AdCSV with 2-(2-thiazolylazo)-p-cresol (TAC), which would equate to a logK'$_{Fe'L}$ of 10.08 mol^{-1} assuming an inorganic side reaction coefficient of 10^{10}. In that same study, the logK'$_{Fe'L}$ found for purified siderophores was 12.12 ± 0.16 mol^{-1}, putting the viral lysates in a different ligand class than siderophores. In a related study in natural waters, Velasquez and colleagues (2011) found logK'$_{Fe'L}$ values of 11.4 to 12.4 mol^{-1} (converted from their reported logK'$_{Fe3+}$ values of 21.4 to 22.4 mol^{-1}) in conjunction with a strong siderophore presence. A similar study in which

bioassays were conducted on natural samples reported $logK'_{Fe'L}$ values of 10.89 to 11.11 mol^{-1} in bacterial presence (converted from their reported $logK'_{Fe3+}$ values of 20.89 to 21.11 mol^{-1}), with siderophore presence confirmed using LC-ESI-MS (Velasquez et al., 2016). While Hassler et al. (2011b) describe EPS as weak ligands of higher relative concentration, quoting $logK'_{Fe'L}$ values as low as 8.7 mol^{-1} (Rue and Bruland, 2001); higher $logK'_{Fe'L}$ values up to ranges similar to siderophores have also been attributed to EPS (Norman et al., 2015). Hassler et al. (2017) expend some effort tying K' to different functional groups and regions but concluded that such metrics lack the detail required to properly designate groups by themselves. In the present study

Taking into account both ligand concentration and binding strength, the reactivity of the ligands ($\alpha_{Fe'L}$) may better reflect the differences in ligand types found in the different cultures (Gledhill and Gerringa, 2017)., $log\alpha_{Fe'L}$ showed near-complete separation between the host species. The relatively high concentrations of Fe-binding organic ligands present in the cultures most likely explains why $log\alpha_{Fe'L}$ values in the present study are considerably higher than those found under natural conditions in the open ocean (Caprara et al., 2016). Alternatively, analytical issues may have played a role. CLE-AdCSV could not be successfully performed in senesced samples as electrochemical consistency could not be reached in the titrations. Changes in speciation must then be inferred from LC-ESI-MS. Ultimately, only a combination of more specific measurements and correlative relationships may yield enough information to elucidate relative contributors to the organic Fe-binding ligand pool (Gledhill and Gerringa, 2017; Hassler et al., 2017; Slagter et al., 2017).

The Ferrioxamine G concentration was well beyond the detection limit in *P. globosa* cultures at 96 h p.i. A contaminantly high concentration of Ferrioxamine G in one of the *P. globosa* controls corresponds to the highest $logK'_{Fe'L}$ value found in those cultures. Given the high K' typically associated with siderophores(Hassler et al., 2017), the high K' may reflect the presence of Ferrioxamine G. Absence of these high concentrations after senescence indicates that Ferrioxamine G is lost or broken down over time. In contrast to *P. Globosa*, Ferrioxamine G was not found in *M. pusilla* cultures at 96 h p.i., and was detected in one post-senescence control of that host. Similarly, Ferrioxamine B was mostly detected in post-senescence *M. pusilla* cultures. This would indicate that the phytoplankton culture, or the community of heterotrophic bacteria endemic to these particular cultures, is determinant in the formation of these ferrioxamines. In *P. globosa*, Ferrioxamine B was only detected at concentrations near the detection limit without a clear disposition between samples. Ferrioxamine E was only found in one *M. pusilla* control, and in higher concentration after senescence. In contrast, Ferrioxamine E was

highest in one *P. globosa* control, and diminished after senescence. Overall, we can identify both production and breakdown processes, which are most strongly tied to the phytoplankton host species.

Ferrioxamine G was found in concentrations an order of magnitude higher than the ranges reported for the open ocean (e.g. Mawji et al., 2008; Boiteau et al., 2016), but only with one phytoplankton host species and only in the (recent) presence of the phytoplankton cells. Additionally, the picomolar concentrations of Ferrioxamines found in our analyses are 1-3 orders of magnitude below [L_t] found electrochemically, and therefore presumably only a small part of the Fe-binding organic ligand pool in these cultures.

Beyond the Ferrioxamines we report on a multitude of siderophore-like substances, i.e. substances in which Fe can be displaced by Gallium (Ga) and bound substances may be detected through the Ga isotope ratio (McCormack et al., 2003). It must be noted that the Ga complexes indicate possible siderophore-like substances, and not all types are detectable (Mawji et al., 2011). Siderophore-like substances were observed with different responses to experiment treatment and the senescence period. Many substances seem to a have a somewhat random presence, occurring in single replicates of the different treatments, sometimes with very large peaks. Overall, the Ga complexes detected were similar at 96 h p.i., and in all treatments diminished after 30 d senescence. This would indicate a loss of siderophore-like substances over time through breakdown or modification, either removing these from the Fe-binding organic ligand pool or possibly changed into other siderophore-like substances (Mawji et al., 2008).

Two substances with lower mass ratios (m/z 386.11 and 414.10) stood out in that these were uniformly present to meaningful levels across treatments and host species but only after dark senescence. This would suggest these substances were produced by the bacteria present. As the bacterial communities were presumably specific to the cultures, these may be very general Fe-binding substances produced by heterotrophic bacteria. A more recalcitrant substance was also observed (m/z 721) in most samples. Senesced *M. pusilla* also reflected the high concentration of Ferrioxamine B (m/z 627.26) reported earlier only in the 96 h p.i. samples, suggesting that it may not have been entirely eliminated as the standard additions would seem to indicate. However, ion counts do not necessarily equate (pico)molar concentrations above the detection level.

Loss factors of Fe-binding organic ligands thus far posited are photochemical degradation (Barbeau et al., 2003; Powell and Wilson-Finelli, 2003b) and topdown control by protists or viral lysis, in turn potentially releasing ligands (Hutchins et al., 1995; Poorvin et al., 2011) as well as modification and

breakdown by protists. However, it is unclear if these processes lead to a removal of the ligands or a modification into ligands of another class or group. For instance, it stands to reason that less than completely recalcitrant substances such as fulvic acids are broken down, the diverse Fe binding sites present in these substances are not necessarily removed from the system. Similarly, modification of siderophores may not necessarily remove their Fe binding properties, but modify them to a point these are shifted into a weaker ligand class. Electrochemistry cannot give insight in such processes due to its inherent "black-box" approach to ligand characterization. Broad spectrum analysis techniques such as the Ga-replacement LC-ESI-MS as used indiscriminately in the present study will be invaluable tools to enhance knowledge gained from electrochemical methods to a point where a complete picture of both specific ligand characterization and strength and kinetics of the redox interactions belying the Fe-binding organic ligand pool.

8.5. Conclusions

In all, an increased total ligand concentration in viral lysates of *P.globosa* shows that the viral shunt not only releases bioavailable Fe to the surrounding seawater (e.g. Poorvin et al., 2004), but also contributes to the Fe-binding organic ligand pool. The comparative lack of such influence from *M. pusilla* may be explained by the small cell size. Ligand classes differ between the two phytoplankton host species in the present study. While a differential in the presence of known siderophores and siderophore-like substances is also observed between host species and treatment in some cases, the relative abundance in comparison to the relatively high [L_t] found in our cultures cannot serve to tie these ligand classes to specific substances. What is evident is that the ligand pool is modified by bacterial both as a loss factor as well as a source of Fe-binding organic ligands, indicating that the viral shunt and bacterial remineralisation work in tandem.

Occurrence of siderophores produced by bacteria present in the different culture treatments are more dependent on the phytoplankton host species than the treatment. Ferrioxamine type siderophores seem to be produced mainly after senescence in *M. pusilla*, whereas they are dominant in the (recent) presence of the living *P. globosa* host. The highest Ferrioxamine G concentrations are reflected in ligand binding strength in one occurrence.

Ga complexes as representatives of potential siderophore-like substances show a uniform loss of these substances after the senescence period, identifying a loss factor of Fe-binding organic ligands. The timescale to study the effect of bacterial modification of Fe-binding organic ligands was chosen to guarantee

sufficient contrast, but it is too long to study specific processes. Further study of siderophore lability and evolution with smaller timescales would be advisable, preferably with larger volumes to increase detection limits and sample interval. Ideally, axenic phytoplankton host cultures with the addition of specific bacteria are used, although this will be very challenging in trace metal clean methodology. Many Ga complex isotopic signatures of siderophore-like substances here detected are thus far unknown. While this opens up a world of complexity to study in detail, this is not unwelcome given the "black box" extent of insight in specific substances thus far derived from established techniques. A combination of techniques shall be the avenue providing most insight going forward, as the new substance-specific techniques cannot convey information on the kinetics of these substances, and electrochemical techniques lack the specificity to characterize the Fe-binding organic ligand pool.
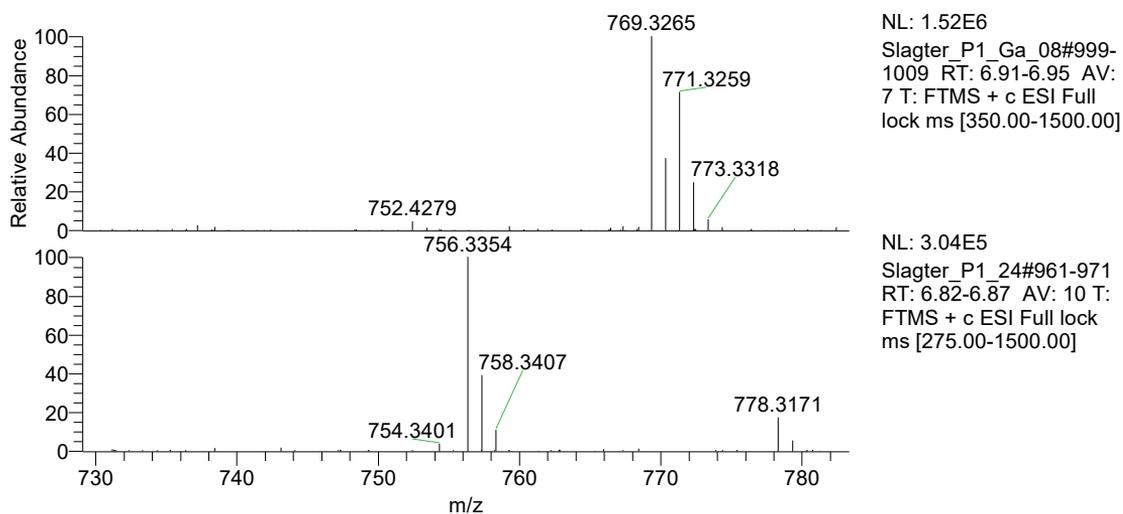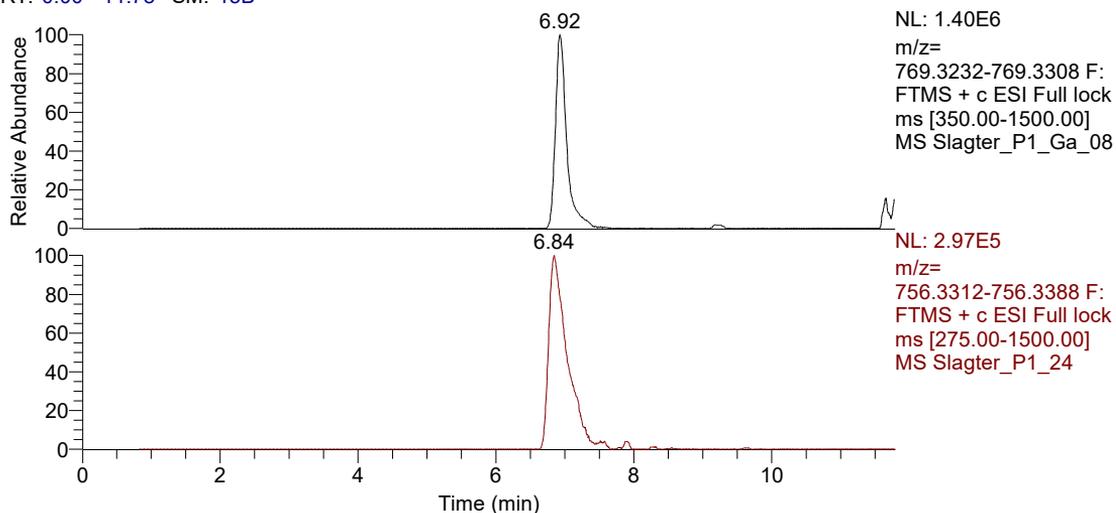
Figure S1 LC-ESI-MS data for a putative siderophore in one *P. globosa* control culture showing (A) the extracted mass chromatogram for the [69]Ga complex and (B) the [56]Fe complex after addition of the respective metal ions to separate aliquots of the sample. Average mass chromatograms obtained at the peak apex for (C) the Ga complex (N=7) showing the distinctive Ga isotopic signature and (D) the Fe complex (N=10) showing the presence of the [54]Fe isotope at 754.3401 (Δ1.995).